

# Renal ischemia/reperfusion-induced cardiac hypertrophy in mice: Cardiac morphological and morphometric characterization

Rogério Cirino-Silva, Fernanda V Kmit, Mayra Trentin-Sonoda, Karina K Nakama, Karine Panico, Juliana M Alvim, Thiago R Dreyer, Herculano Martinho-Silva and Marcela S Carneiro-Ramos

## Abstract

**Background:** Tissue remodeling is usually dependent on the deposition of extracellular matrix that may result in tissue stiffness and impaired myocardium contraction.

**Objectives:** We had previously demonstrated that renal ischemia/reperfusion (I/R) is able to induce development of cardiac hypertrophy in mice. Therefore, we aimed to characterize renal I/R-induced cardiac hypertrophy.

**Design:** C57BL/6J mice were subjected to 60 minutes' unilateral renal pedicle occlusion, followed by reperfusion (I/R) for 5, 8, 12 or 15 days. Gene expression, protein abundance and morphometric analyses were performed in all time points.

**Results:** Left ventricle wall thickening was increased after eight days of reperfusion ( $p < 0.05$ ). An increase in the number of heart ventricle capillaries and diameter after 12 days of reperfusion ( $p < 0.05$ ) was observed; an increase in the density of capillaries starting at 5 days of reperfusion ( $p < 0.05$ ) was also observed. Analyses of MMP2 protein levels showed an increase at 15 days compared to sham ( $p < 0.05$ ). Moreover, TGF- $\beta$  gene expression was downregulated at 12 days as well TIMP 1 and 2 ( $p < 0.05$ ). The Fourier-transform infrared spectroscopy analysis showed that collagen content was altered only in the internal section of the heart ( $p < 0.05$ ); such data were supported by collagen mRNA levels.

**Conclusions:** Renal I/R leads to impactful changes in heart morphology, accompanied by an increase in microvasculature. Although it is clear that I/R is able to induce cardiac remodeling, such morphological changes is present in only a section of the heart tissue.

## Keywords

Cardiac hypertrophy, extracellular matrix, renal ischemia–reperfusion, Fourier-transform infrared spectroscopy, Cavalieri's principle

Date received: 18 July 2016; accepted: 22 December 2016

## Introduction

Cardiac hypertrophy (CH) is usually accompanied by fibroblast proliferation and synthesis of extracellular matrix (ECM), which forms the structural backbone of the heart. ECM is composed of a macromolecule complex that includes collagens, proteoglycans and elastic fibers.<sup>1,2</sup> Besides its structural functions, ECM also provides a molecular microenvironment for cell differentiation, growth and angiogenesis.<sup>3</sup> Most extracellular protein matrixes are minimally expressed in normal adult hearts but they are intensely upregulated after tissue injury.<sup>4</sup>

Regulation of ECM is based on a dynamic balance between the synthesis of collagen, degradation by matrix metalloproteinases (MMPs, matrixins), ADAMTS proteinases (a distegrin-like and metalloproteinase domain

Centro de Ciências Naturais e Humanas, Universidade Federal do ABC, Brazil

### Corresponding author:

Marcela S Carneiro-Ramos, Centro de Ciências Naturais e Humanas, Bloco A, Torre 3, Santo Andre, SP 09210-170, Brazil.  
Email: marcela.ramos@ufabc.edu.br



with thrombosposin type 1 repeat) and tissue inhibitors of MMPs (TIMPs).<sup>5</sup>

On the other hand, development of CH is a much more complex phenomenon than its definition suggests. Increase of cardiac mass may be mediated by fibroblasts proliferation and hypertrophy of individual cardiomyocytes, which occurs in response to pathological conditions.<sup>6,7</sup> For instance, postnatal hypertrophy induced by circulatory hormones may lead to increased contractile units deposition in cardiomyocytes and remodeling of ECM to a new functional scenario.

Patients with renal insufficiency have a higher risk of developing cardiovascular diseases (CVD), representing 45% of the causes of death in patients undergoing hemodialysis treatment.<sup>8</sup> Additionally, our group had previously demonstrated that unilateral renal ischemia/reperfusion (I/R) is able to generate renal lesion, followed by systemic sterile inflammation, resulting in the development of CH in mice.<sup>9</sup>

Considering that (1) renal I/R leads to CH and (2) collagen deposition plays a major role in cardiac remodeling, the aim of the present study was to characterize the CH induced by renal I/R regarding changes in cardiac ECM and morphometric parameters.

## Methods

### Animal procedures

All surgical procedures and protocols were performed in accordance with the Ethical Principles in Animal Research set forth by the Brazilian College of Animal Experimentation and were approved by the Biomedical Sciences Institute/USP Ethics Committee for Animal Research (Book 20, Protocol 36, p. 68). Male C57bl/6J mice, five to eight weeks old (22–28 g) were obtained from the University of São Paulo, Institute of Biomedical Sciences, in São Paulo, Brazil. Mice were given free access to standard mice chow and water until the time of the experiment and were housed in a temperature and light-controlled environment (24°C; 12/12-h light/dark cycle).

### Renal I/R

Renal I/R protocol was performed as previously described by our group and Feitoza et al.<sup>9,10</sup> Mice were anesthetized using ketamine/xylazine. An abdominal incision was made and left renal pedicle was exposed and then was occluded by a steel clamp (DL Micof, São Paulo); after 60 minutes of occlusion, the steel clamp was removed, followed by reperfusion for 5, 8, 12 and 15 days. Sham operated was subject to abdominal incision but not to pedicle occlusion procedure.

### Morphometric parameters and morphology analysis of heart

The weight of the heart was assessed by an analytic scale (Denver Instrument®) and measures of three axes were made – length, weight and thickness – using images acquired by Motic camera and analyzed by Motic Images Plus 2.0. Right and left atria were removed along with great vessels, and hearts were weighted once again. After dividing hearts into three to four transversal slices of 3 mm (Figure S1(a)), following Cavalieri's method,<sup>11</sup> new images were acquired. These images were utilized to assess the thickness of the left ventricle wall, right ventricle wall, and interventricular septum (Figure S1(b)). Left ventricle volume was estimated by weight/density = volume ( $\frac{m}{d} = V$ ) formula, considering heart tissue density as 1.06 g/cm<sup>3</sup>, as previously described by Bruel et al.<sup>12</sup>

Histological examination was performed as previously described (p. 51)<sup>9</sup> where four sections of each slide were randomly chosen and utilized to count and measure the diameter of the capillaries. The density of the capillaries was calculated as a ratio of capillaries by cardiomyocytes number. Pictures were acquired in Nikon® E-2000 microscope. Data acquisition was performed using an independent software based on MATLAB R2011a and toolbox image processing, developed by Oliveira and Nascimento from the Universidade Federal do ABC.

### Gene expression

RNA from heart ventricles was extracted using Trizol® technique, following manufacturer's instructions, RNA was quantified using NanoDrop™ Lite (Thermo Scientific) and 2 µg of total RNA was subjected to a reverse transcriptase reaction, and as a final product, we obtained the cDNA that was used to perform real-time PCR (Stratagene® Mx3005P). The levels of mRNA of Collagen I, Collagen III, FGF-2, MMP2, TGF-β, TIMP1, TIMP2 and cyclophilin A were analyzed. Primer sequences utilized can be found in Table 1.

### Protein expression

Total protein from heart was obtained using radioimmunoprecipitation assay (RIPA) lysis buffer. Protein concentrations were determined by using the BCA kit (Thermo Scientific). Forty micrograms of total protein were resolved by electrophoresis on 5% stacking/15% polyacrylamide–sodium dodecyl sulfate gels, and the resolved proteins were transferred to nitrocellulose membrane (Bio-Rad). The membrane was stained with Ponceau solution, to demonstrate that the protein concentration was similar in the different lanes. The membrane was then washed with TBST (Tris 50 mM,

**Table 1.** List of primers.

Gene	5'–3'	3'–5'
Collagen I	GCCAAGAAGACATCCCTGAA	GGTTGGGACAGTCCAGTTCT
Collagen III	GCACAGCAGTCCAACGTAGA	GGCAGTCTAGTGGCTCCTCA
Cyclofilin-a	AGCATACAGGTCTGGCATC	AGCTGTCCACAGTCGGAAAT
FGF-2	GCCGTCCATCTTCCTTCATA	CCACACGTCAAACACTACAACCTCC
MMP2	GTCGCCCCTAAAACAGACAA	GGTCTCGATGGTGTCTGGT
TGF- $\beta$	ACGTCAGACATTTCGGGAAGC	ACCAAGGTAACGCCAGGAAT
TIMP1	CTTGGGACCTCAAAGAGCAG	CAAGCCAGGAGGAGACAGAC
TIMP2	CTTGGGACCTCAAAGAGCAG	CAAGCCAGGAGGAGACAGAC

NaCl 150 mM, pH 7.5 and Tween-20 2%) for 10 min at room temperature. Primary antibodies were incubated overnight at 4°C [anti-MMP2 (1:500) and GAPDH (1:1000)]. After washing the membranes, the secondary antibody conjugated with peroxidase (Jackson) at a 1:10,000 dilution in TBST was added for 1 h at room temperature. The membranes were washed again with TBST and incubated with ECL detection reagents (Amersham Biosciences), which produced a chemiluminescent signal that was detected by exposure to X-ray film. The protein bands were quantified by densitometry using Image J<sup>®</sup>.

### Cardiac ECM deposition analysis by Fourier-transform infrared spectroscopy

Left ventricle samples of each group were cut into three different slices: intern (1), medial (2), and external (3) sections (Figure 5(a)) and placed in a platinum sample holder. Fourier-transform infrared (FT-IR) absorption spectra for each slice were acquired in a Varian FT-IR 610 micro-spectrometer (Ge-ATR mode). The measurements were performed on four different points (200 scans per sample; 400 scans for background) spectral resolution of 4 cm<sup>-1</sup>. Each spectrum was manually baseline corrected with Fityk software.<sup>13</sup>

### Statistics

Data are expressed as mean  $\pm$  SEM. Groups were compared using one-way analysis of variance (ANOVA) followed by Bonferroni test. A  $p < 0.05$  was considered significant. To perform the FTIR spectroscopy analysis, the regions 1137–1189 cm<sup>-1</sup> and 1600–1680 cm<sup>-1</sup> were analyzed once collagen types I and III could be differentiated through these regions.<sup>14</sup> The spectra were normalized by their integrated area under the spectral curves in the range 900–1800 cm<sup>-1</sup> and 2530–3600 cm<sup>-1</sup>, and the regions ranging between 1137–1189 cm<sup>-1</sup> and 1600–1680 cm<sup>-1</sup> were analyzed

by their integrated areas to verify the amounts of collagens I and III present in the sample. Integrated areas were compared by ANOVA and Tukey post ANOVA test when the data were normally distributed, or Kruskal–Wallis and Mann–Whitney tests when data were not following a normal distribution.

## Results

### Effects of renal I/R in cardiac morphology

To characterize CH generated by renal I/R, the external morphology was analyzed. After perfusion of heart tissue, measurements of height, length and circular diameter were taken (Figure 1(a) to (d)). Although our group had previously found that renal I/R is able to induce CH,<sup>9</sup> external morphology analysis showed no significant changes among groups. On the other hand, renal I/R was able to induce changes in the left ventricle wall, since thickening was observed after eight days of reperfusion, sustained until 15 days (Figure 2(a)). The right ventricle wall thickness of I/R mice showed no significant differences when compared to sham, although there is a clear tendency to increase (Figure 2(b)). Additionally, a thickening of the inter-ventricular septum at the first and last time point studied (5 and 15 days, respectively – Figure 2(c)) was also observed. Left ventricle volume analysis, assessed by Bruel and Niengard method, showed a significant increase in the 15-day group (Figure 2(d)).

### Renal I/R effects in angiogenesis

I/R was able to augment abundance of capillaries after 12 days of reperfusion (Figure 3(a)); additionally, the diameter of the capillaries was increased when compared to sham (Figure 3(b)), starting at 5 days and being sustained until 15 days. Such changes were also observed in the density of the capillaries (Figure 3(c)), and increased in all time points from 5 to 15 days.

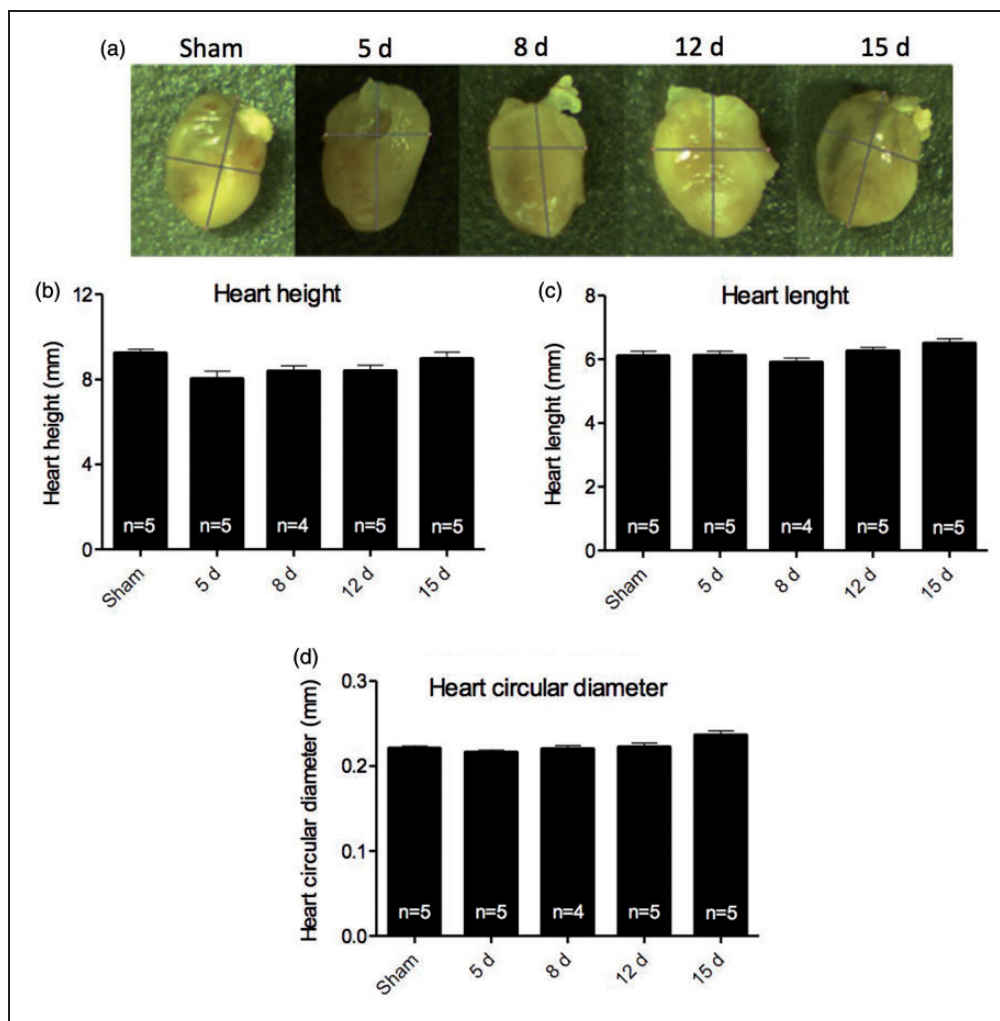


**Figure 1.** External heart's morphology characterization. (a) representative images from hearts were obtained for each group. (b) Heart height. (c) Heart length and (d) heart circular diameter obtained. Measurements show no significant difference among the groups. Data are expressed as mean  $\pm$  SEM, \* vs. sham,  $p < 0.05$ .

### Cardiac ECM in renal I/R model

Considering that renal I/R model was able to induce an increase in cardiac mass, we evaluated the effects of I/R on ECM remodeling. First, we analyzed MMP2 gene expression and protein levels in heart tissue after kidney injury. Although mRNA levels were decreased at 8 and 12 days, protein levels of MMP2 showed an increase after 15 days of reperfusion when compared to sham animals (Figure 4(a) and (b),  $p < 0.05$ ). Moreover, the specific inhibitor of MMP2, TIMP1, appeared diminished in the 12-day group (Figure 4(c)). In addition, another MMP inhibitor, TIMP2 is also diminished after 12 days of reperfusion (Figure 4(d),  $p < 0.05$ ). ECM deposition is not only regulated by MMPs and TIMPs, but it is also a target for growth factors; therefore, we evaluated gene expression of TGF- $\beta$  and FGF-2.

TGF- $\beta$  mRNA levels were decreased after 12 days of reperfusion (Figure 4(g),  $p < 0.05$ ), whereas the analysis of FGF-2 mRNA levels did not show any significant changes, despite a clear trend to downregulation in all I/R groups. Furthermore, collagens I and III mRNA levels were unaltered (Figure 4(e) and (f)).

The levels of collagen types I and III in heart tissue samples were also evaluated through FTIR. Figure 5(b) shows the average spectra for sham, 12-day and 15-day groups. The fingerprint region ( $800\text{--}1800\text{ cm}^{-1}$ ) presented the well-known vibrational modes of DNA, RNA, amino acids and sugars. It is important to claim attention to the behavior of  $1170\text{ cm}^{-1}$  band and  $1600\text{--}1720\text{ cm}^{-1}$  spectral region (inset of Figure 5(b)). The former relates to the C–O stretching vibration of collagen I while the latter is a spectral window where Amide I sub-bands related to peptidic bond vibrations. These sub-bands have pieces of information concerning

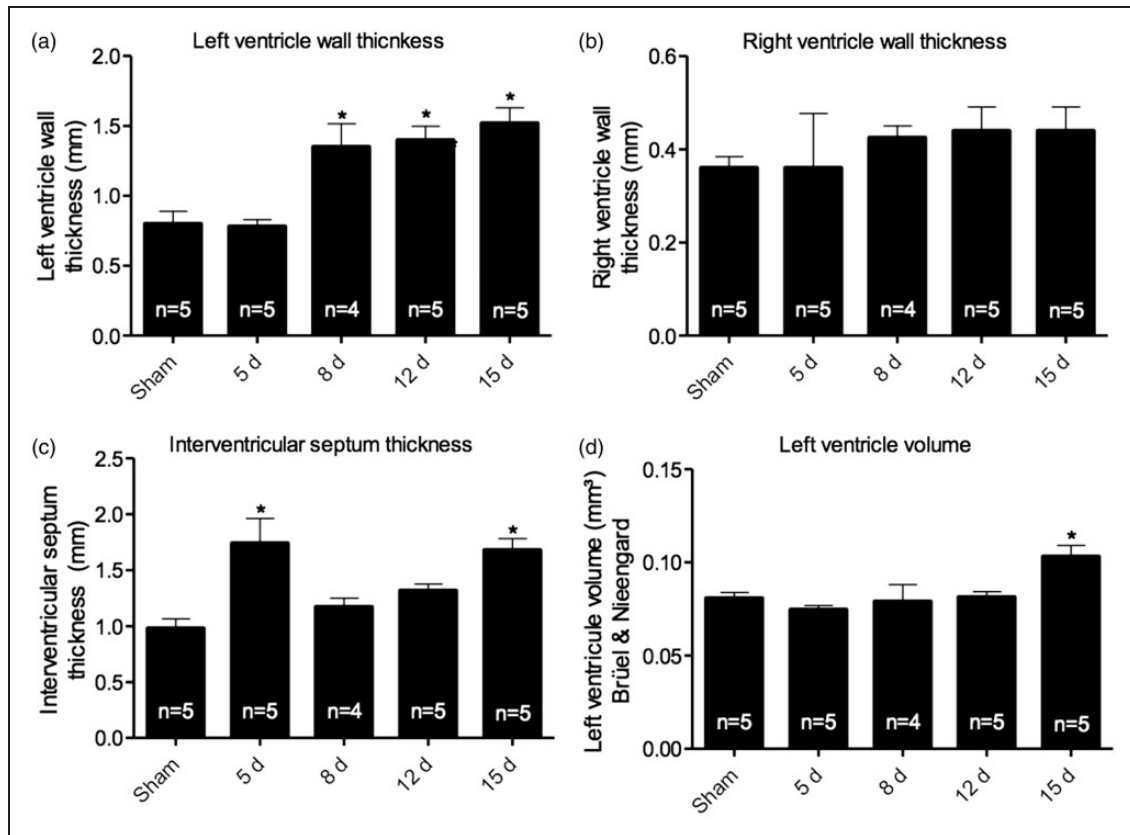


**Figure 2.** Data obtained via Cavalieri's methods. (a) Left ventricle wall thickness showing increase after 8 days of reperfusion. (b) Right ventricle wall thickness shows no significant changes. When analyzed (c) interventricular septum thickness, a significant increase in groups 5 and 15 days was observed (d) Left ventricle volume assessed by Bruel and Nieengard method's show increase only in the 15-day group. Data are expressed as mean  $\pm$  SEM, n = number of samples. \* vs. sham,  $p < 0.05$ .

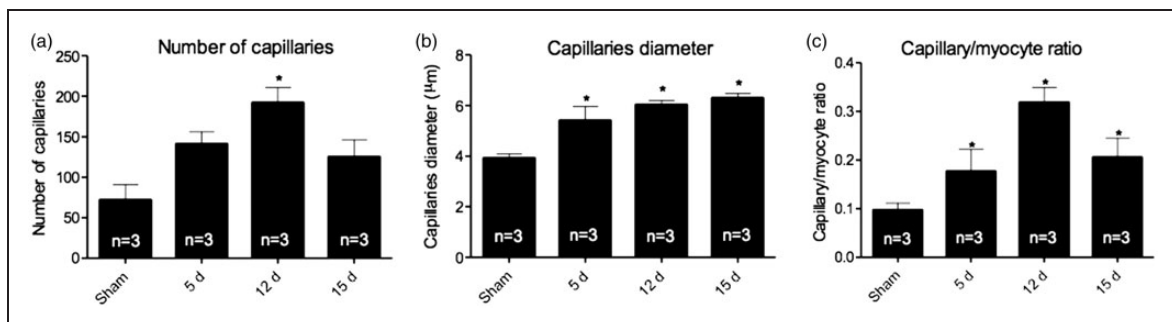


**Figure 3.** Angiogenesis parameters were analyzed using (a) number of capillaries, which show increase in 12-day group (b) capillaries diameter, increasing after 5 days of reperfusion and being sustained until 15 days, that was not reflect in (c) capillaries density, which showed an increase in all groups of reperfusion. Data expressed as mean  $\pm$  SEM, n = number of samples. \* vs. sham,  $p < 0.05$ .

the conformational state of the proteins, especially collagen. At first glance, the average spectral intensities indicate that the collagen I content gradually increased from sham to the 15-day group. In the range of frequencies 1137–1189  $\text{cm}^{-1}$ , data did not follow a normal distribution and the Kruskal–Wallis test showed no differences of the integrated areas under the different

samples. The same results were obtained for collagen III (1600–1680  $\text{cm}^{-1}$ ). A semi-quantitative analysis was performed by the analysis of the ratio of the integrated areas of 1600–1680  $\text{cm}^{-1}$  and 1137–1189  $\text{cm}^{-1}$  spectral region. The data indicated that the 15-day group presented a higher collagen III content compared to other groups.

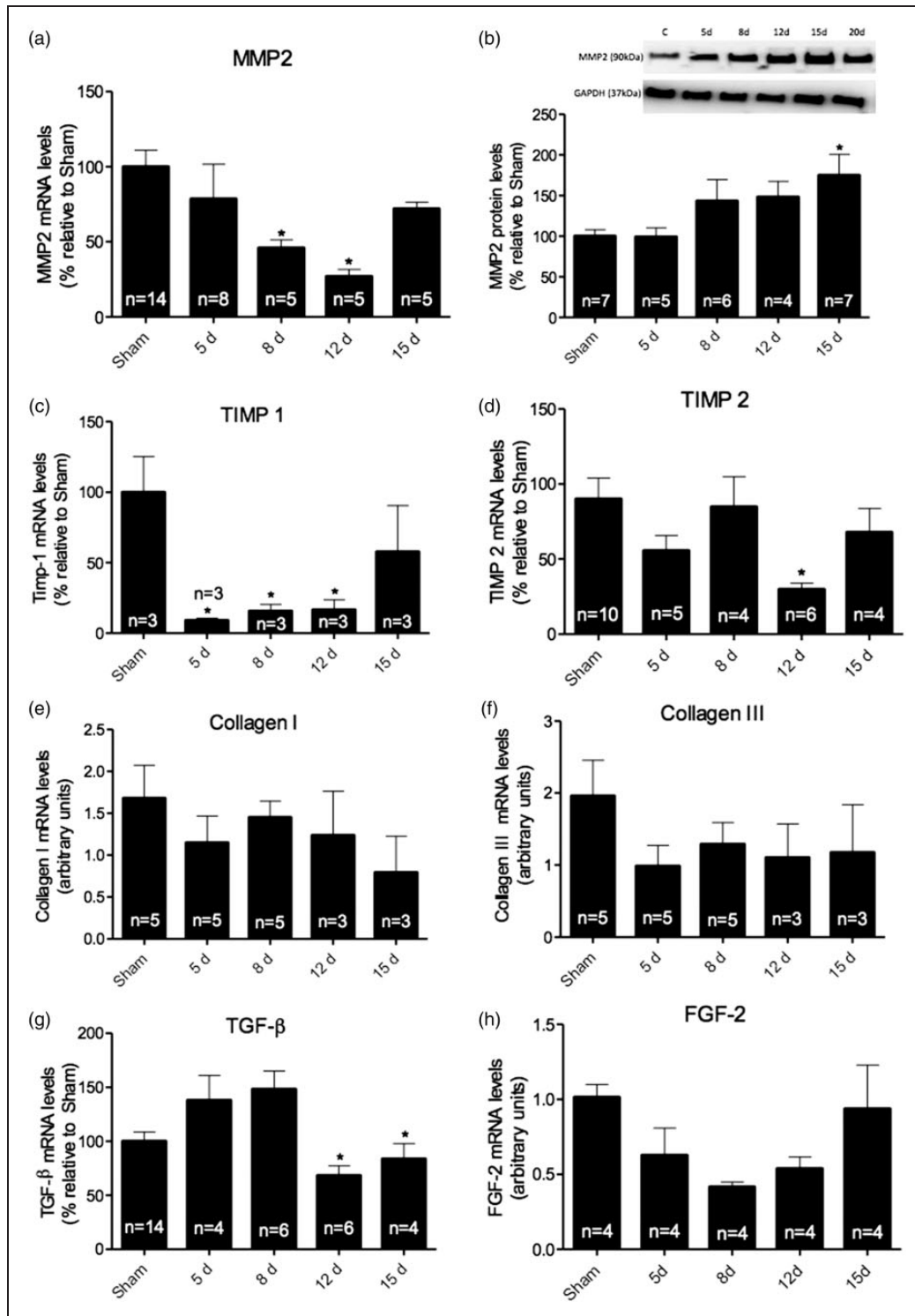


**Figure 4.** To assess cardiac remodeling, mRNA and protein levels of key molecules in extracellular matrix deposition were measured in the cardiac tissue. (a) mRNA levels of MMP2 analysis showed a decrease between 8 and 12 days of reperfusion. (b) Protein levels showed an increase in 15-day group. Regulators of MMPs, (c) TIMP1 mRNA levels showed a decreased in almost all groups, except for group 15 days, while (d) TIMP2 mRNA levels were decreased only in 12-day group. The mRNA levels of (e) collagen I and (f) collagen III were also analyzed, since they are essential to extracellular matrix deposition; however, no significant changes were observed. Additionally, the levels of mRNAs of (g) TGF- $\beta$  were analyzed in heart tissue, showing significant decrease between 12 and 15 days. (h) FGF-2 levels were also analyzed.

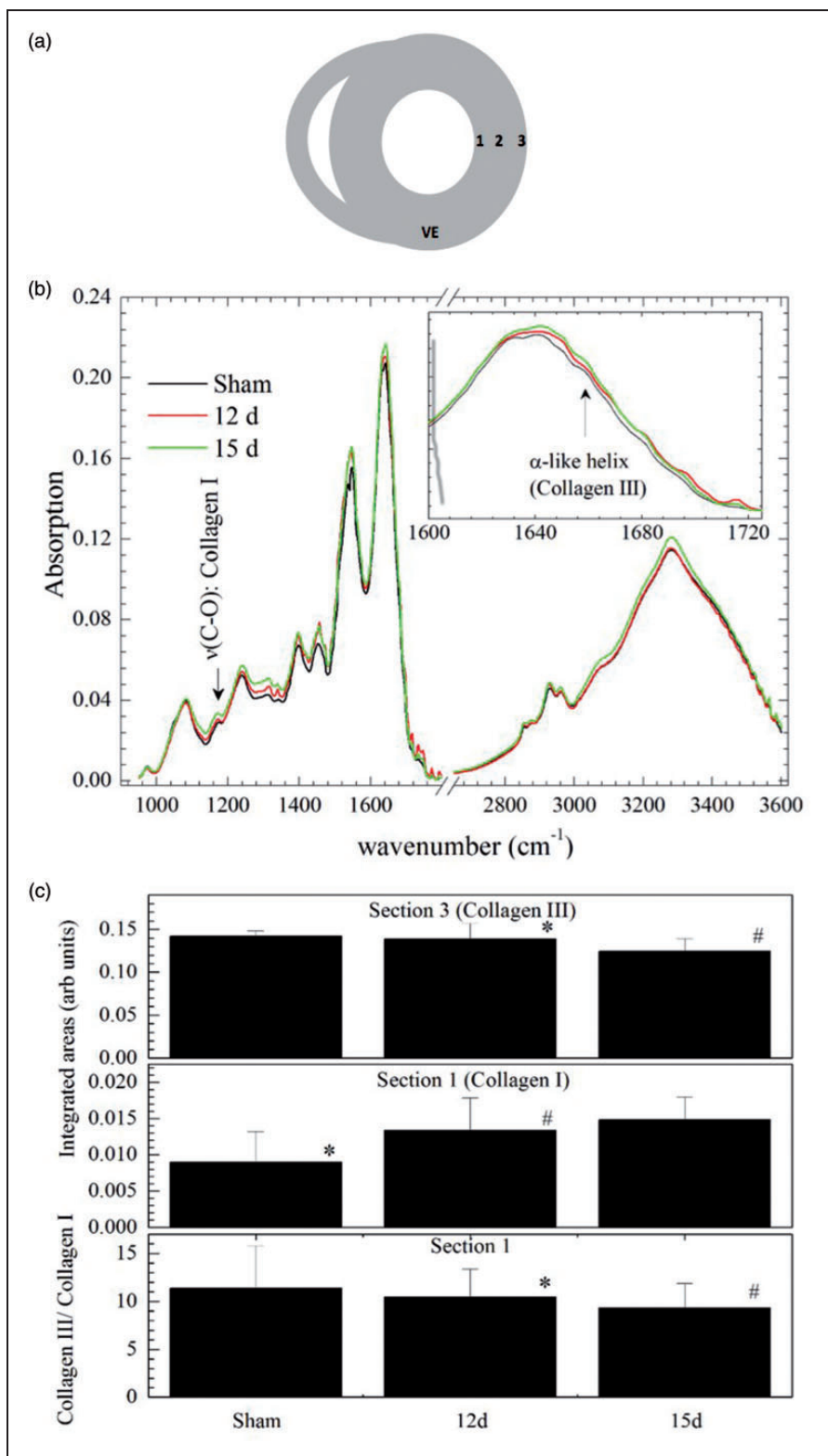


**Figure 5.** FTIR analysis of the integrated areas. (a) Representative image of areas utilized to perform FTIR measurements. (b) Representative image of absorption spectra, showing different peaks. (C(i)) Collagen III content at external section, (C(ii)) collagen I content at internal section and (C(iii)) collagen III/collagen I content at internal section. Data expressed in mean  $\pm$  SD. \* $p < 0.0303$ ; # $p < 0.0467$ .

In relation to external section, the analysis of the integrated areas showed differences for collagen III, 1600–1680  $\text{cm}^{-1}$  (Figure 5(a)), demonstrating a decrease in the samples for the 15-day group compared to sham and 12-day group which implies higher collagen III content for this specific group. The regions of collagen I (1137–1189  $\text{cm}^{-1}$ ) and the values of the ratio (1600–1680/1137–1189  $\text{cm}^{-1}$ ) showed no differences among the groups.

Regarding the internal section, the integrated area in the spectral range 1137–1189  $\text{cm}^{-1}$  (collagen I) for the 12-day and the 15-day groups presented statistically significant difference compared to the sham group (Figure 5(c)). This implies that collagen I content continuously increased as within time of reperfusion. Otherwise, the spectral region between 1600 and 1680  $\text{cm}^{-1}$  (collagen III) did not show significant variation. Thus, in this section tissue, the collagen III content was almost constant. The ratio of the integrated areas presented non-normal distribution. The differences pointed out by Kruskal–Wallis/Mann–Whitney test ( $p = 0.013$ ) could be observed in Figure 5(c) and reflects the collagen I content variations. In relation to medial section, there is no statistical evidence (ANOVA test) for spectral differences. Taken together, we are able to infer that the total collagen content did not alter in whole heart.

## Discussion

In the present study, we hypothesized that renal I/R would be able to change deposition of ECM components. Herein, we have shown that CH induced by renal I/R is not accompanied by total collagen content alterations.

Heart and kidney diseases were considered as separated ailments for a long time; however, a trend to integrative science has been observed in the latest years, and a consequence of such event was the discovery of cardiorenal syndrome, characterized by a complex and multifactorial interaction between both organs.<sup>15</sup> Renal failure is followed by cardiovascular alterations and is framed in a subtype of cardiorenal syndrome. The coexistence of CVDs and kidney failure has several implications, such as decreased survival rates.<sup>16,17</sup>

Regarding the cardiac tissue, since heart external morphometric parameters were not altered, and left ventricle wall thickness was increased after eight days of reperfusion ( $p < 0.05$ ), it was possible to infer that a concentric type of CH is installed after 12 days of reperfusion. This result corroborates others in the literature, as well as previous results from our lab, showing that inflammatory cytokines were able to induce an increase in cardiac mass after renal I/R.<sup>9,18</sup>

Nonetheless, we had previously shown that CH induced by renal I/R is accompanied by increased

transverse cardiomyocyte diameter,<sup>9</sup> without alterations on blood pressure and heart frequency (data not published), characterizing a nonstandard model of CH. In this model, inflammation seems to be a key participant in cardiac mass increase, since lack of TLR2 or TLR4 is sufficient to prevent development of CH ( $p = 51$ ).<sup>9</sup>

CH is usually followed by increase in heart tissue vascularity, since myocardial expansion is accompanied by a greater demand in oxygen and nutrients; therefore, an increase in the number of capillaries is necessary to supply the raising demand.<sup>19</sup> In our model, the number of capillaries, diameter and density were increased ( $p < 0.05$ ), corroborating previous studies on pathological cardiac remodeling.<sup>20</sup>

The cardiac tissue structure depends on the number and size of fibroblasts and cardiomyocytes. Once the number of fibroblast increases, it directly reflects on the alterations of ECM components, mainly collagens I, III and matrix metalloproteinases.<sup>4</sup> Therefore, we have evaluated the effect of I/R protocol in MMP2 and collagen levels in all the time points studied. Although the results showed a significant decrease in MMP2 gene expression between 8 and 12 days ( $p < 0.05$ ), protein levels were only increased after 15 days ( $p < 0.05$ ). In parallel, we observed a decrease in gene expression of TIMP1 in the 12-day group when compared with control animals ( $p < 0.05$ ), suggesting an augmented activity towards ECM degradation.

Although cardiovascular inflammation induced by renal I/R is not completely understood, the role of inflammation on ECM modulation, after myocardial infarction (MI), is well characterized.<sup>21</sup> After about 1 h of ischemia, cardiomyocytes undergo necrosis accompanied by activation of toll-like receptors, reactive oxygen species synthesis and increase in cytokine levels. Neutrophils are the first immunity cells to be recruited and after about three days, macrophages remove necrotic cardiomyocytes and apoptotic neutrophils.<sup>22</sup> Macrophages activate fibroblasts through TGF- $\beta$  dependent manner,<sup>23</sup> which may suppress the inflammatory response stimulating fibroblasts' conversion into myofibroblasts.<sup>24</sup> After one week of MI, collagens I and III are deposited in cardiac tissue promoting fibrosis.<sup>25</sup> When the reperfusion is reopened, infiltration of the inflammatory cells is accelerated and amplified, impairing left ventricle function.<sup>26</sup> Surprisingly, the mRNA levels of TGF- $\beta$  were down-regulated after 12 days of reperfusion ( $p < 0.05$ ). Along with results from MMP analysis and collagen gene expression, it was not possible to infer whether I/R induced fibrosis in the heart tissue.

Several studies have been correlating the structural alterations of collagen to pathologies development.<sup>27,30–31</sup>

Here, we used FTIR spectroscopy to assess the collagen content alterations in different sections of the heart tissue. Even though there are other methods for collagen analysis, there are limitations in all of them, such as sensibility, precision and capacity to evaluate molecular structure.<sup>28</sup> We observed a bland alteration of collagen content in all the three sections studied; still the global analysis showed that renal I/R protocol was not able to change collagen I and III levels at the same time. On the other hand, we could detect an increase in collagen I content in section I ( $p < 0.05$ ), the internal section, which is directly in contact with the circulating cytokines.

The ECM turnover occurs during cardiac remodeling; even so, the mechanisms involved in controlling the balance between production and degradation are not fully understood.<sup>29</sup> Even though we have observed changes in expression of molecules involved in ECM deposition, it remains unclear whether they have a substantial participation in cardiac remodeling induced by renal I/R. A further investigation is necessary to elucidate the mechanisms controlling the suppression of inflammatory signals and the triggering of fibroblasts proliferation in our model. Likewise, we have performed studies involving an animal model, and clinical investigations are essential for a better understanding of I/R effects in cardiac remodeling.

Nevertheless, our data suggest that systemic inflammation is able to modulate cardiac tissue structure, differently regulating collagen content in distinct sections of the heart tissue in mice subject to renal I/R.

#### Declaration of conflicting interests

The author(s) declared no potential conflicts of interest with respect to the research, authorship, and/or publication of this article.

#### Funding

The author(s) disclosed receipt of the following financial support for the research, authorship, and/or publication of this article: This study was supported by FAPESP agency (grants N. 2008/1015-4 and 2015/19107-5) and Brazilian National Research Council (CNPq, grant 481034/2012-9).

#### Ethical approval

None.

#### Guarantor

Marcela S Carneiro Ramos.

#### Contributorship

Rogério Cirino-Silva and Fernanda V Kmit have equal contribution to the work.

#### Supplemental Material

Supplementary material for this paper can be found at <http://journals.sagepub.com/doi/suppl/10.1177/2048004016689440>.

#### References

1. Berk BC, Fujiwara K and Lehoux S. ECM remodeling in hypertensive heart disease. *J Clin Investigat* 2007; 117: 568–575.
2. Creemers EE and Pinto YM. Molecular mechanisms that control interstitial fibrosis in the pressure-overloaded heart. *Cardiovasc Res* 2011; 89: 265–272.
3. Weber KT, Sun Y, Tyagi SC, et al. Collagen network of the myocardium: function, structural remodeling and regulatory mechanisms. *J Mol Cell Cardiol* 1994; 26: 279–292.
4. Frangogiannis NG. Matricellular proteins in cardiac adaptation and disease. *Physiol Rev* 2012; 92: 635–688.
5. Pedersen ME, Vuong TT, Ronning SB, et al. Matrix metalloproteinases in fish biology and matrix turnover. *Matrix Biol* 2015; 44–46: 86–93.
6. Heineke J and Molkenin JD. Regulation of cardiac hypertrophy by intracellular signalling pathways. *Nat Rev Mol Cell Biol* 2006; 7: 589–600.
7. Maillet M, van Berlo JH and Molkenin JD. Molecular basis of physiological heart growth: fundamental concepts and new players. *Nat Rev Mol Cell Biol* 2013; 14: 38–48.
8. Harmankaya O, Akalin N, Akay H, et al. Comparison of risk factors for cardiovascular disease in hemodialysis and peritoneal dialysis patients. *Clinics* 2015; 70: 601–605.
9. Trentin-Sonoda M, da Silva RC, Kmit FV, et al. Knockout of toll-like receptors 2 and 4 prevents renal ischemia-reperfusion-induced cardiac hypertrophy in mice. *PLoS One* 2015; 10: e0139350.
10. Feitoza CQ, Goncalves GM, Semedo P, et al. Inhibition of COX 1 and 2 prior to renal ischemia/reperfusion injury decreases the development of fibrosis. *Mol Med* 2008; 14: 724–730.
11. Gundersen HJ, Bendtsen TF, Korbo L, et al. Some new, simple and efficient stereological methods and their use in pathological research and diagnosis. *APMIS* 1988; 96: 379–394.
12. Bruel A, Oxlund H and Nyengaard JR. The total length of myocytes and capillaries, and total number of myocyte nuclei in the rat heart are time-dependently increased by growth hormone. *Growth Hormone IGF Res* 2005; 15: 256–264.
13. Wojdyr M. Fityk: a general-purpose peak fitting program. *J Appl Crystallogr* 2010; 43: 1126–1128.
14. Belbachir AN, Hofstatter M, Litzberger M, et al. Performance evaluation of the ultra high-speed synchronous arbitration for transient pixels' events. In: *2009 IEEE international conference on industrial technology, vols 1–3*, 2009, pp.6–9. New York: IEEE.
15. Bongartz LG, Braam B, Gaillard CA, et al. Target organ cross talk in cardiorenal syndrome: animal models. *Am J Physiol Renal Physiol* 2012; 303: F1253–F1263.

16. Anavekar NS, McMurray JJ, Velazquez EJ, et al. Relation between renal dysfunction and cardiovascular outcomes after myocardial infarction. *N Engl J Med* 2004; 351: 1285–1295.
17. Damman K, Navis G, Voors AA, et al. Worsening renal function and prognosis in heart failure: systematic review and meta-analysis. *J Card Fail* 2007; 13: 599–608.
18. Mir SA, Chatterjee A, Mitra A, et al. Inhibition of signal transducer and activator of transcription 3 (STAT3) attenuates interleukin-6 (IL-6)-induced collagen synthesis and resultant hypertrophy in rat heart. *J Biol Chem* 2012; 287: 2666–2677.
19. Riley PR and Smart N. Vascularizing the heart. *Cardiovasc Res* 2011; 91: 260–268.
20. Anversa P and Capasso JM. Loss of intermediate-sized coronary arteries and capillary proliferation after left ventricular failure in rats. *Am J Physiol* 1991; 260: H1552–H1560.
21. Frangogiannis NG, Smith CW and Entman ML. The inflammatory response in myocardial infarction. *Cardiovasc Res* 2002; 53: 31–47.
22. Lamberti Y, Perez Vidakovic ML, van der Pol LW, et al. Cholesterol-rich domains are involved in *Bordetella pertussis* phagocytosis and intracellular survival in neutrophils. *Microb Pathog* 2008; 44: 501–511.
23. Sun Y, Zhang JQ, Zhang J, et al. Cardiac remodeling by fibrous tissue after infarction in rats. *J Lab Clin Med* 2000; 135: 316–323.
24. Wynn TA. Cellular and molecular mechanisms of fibrosis. *J Pathol* 2008; 214: 199–210.
25. Jougasaki M, Tachibana I, Luchner A, et al. Augmented cardiac cardiotrophin-1 in experimental congestive heart failure. *Circulation* 2000; 101: 14–17.
26. Jourdan-Lesaux C, Zhang J and Lindsey ML. Extracellular matrix roles during cardiac repair. *Life Sci* 2010; 87: 391–400.
27. Prox J, Arnold P and Becker-Pauly C. Meprin alpha and meprin beta: procollagen proteinases in health and disease. *Matrix Biol* 2015; 44–46: 7–13.
28. Fritschy JM. Is my antibody-staining specific? How to deal with pitfalls of immunohistochemistry. *Eur J Neurosci* 2008; 28: 2365–2370.
29. Ghosh AK and Vaughan DE. PAI-1 in tissue fibrosis. *J Cell Physiol* 2012; 227: 493–507.
30. Cheheltani R, Rosano JM, Wang B, et al. Fourier transform infrared spectroscopic imaging of cardiac tissue to detect collagen deposition after myocardial infarction. *J Biomed Opt* 2012; 17: 056014.
31. Belbachir K, Noreen R, Gousspillou G, et al. Collagen types analysis and differentiation by FTIR spectroscopy. *Analy Bioanal Chem* 2009; 395: 829–837.